NBSIR 80-2175

# Analysis of the Shape of the Far-Infrared Spectra of $H_2$ -$H_2$ and $H_2$ -He Collisions

E. Richard Cohen

Rockwell International Science Center
Thousand Oaks, CA 91360

and

George Birnbaum

National Measurement Laboratory
U.S. Department of Commerce
National Bureau of Standards
Washington, DC 20234



April 1981

Prepared for the Jet Propulsion Laboratory, California Institute of Technology

NBSIR 80-2175

# ANALYSIS OF THE SHAPE OF THE FAR-INFRARED SPECTRA OF $H_2$-$H_2$ AND $H_2$-He COLLISIONS

E. Richard Cohen

Rockwell International Science Center
Thousand Oaks, CA 91360

and

George Birnbaum

National Measurement Laboratory
U.S. Department of Commerce
National Bureau of Standards
Washington, DC 20234

April 1981

Prepared for the Jet Propulsion Laboratory, California Institute of Technology.


U.S. DEPARTMENT OF COMMERCE, Malcolm Baldrige, *Secretary*
NATIONAL BUREAU OF STANDARDS, Ernest Ambler, *Director*

## Abstract

The collision-induced far-infrared spectra due to $H_2$-$H_2$ and $H_2$-He collisions have been previously measured in the range 20 to 900 $cm^{-1}$ at 77.4, 195 and 292 K.[1] These spectra are fitted with a semi-empirical line shape and the parameters in the shape function are evaluated. The accuracy of these fittings is discussed. The zeroth and first spectral moments for the isotropic overlap translational spectrum due to $H_2$-He collisions are obtained and give a value for the range parameter in the induced-dipole function in good agreement with that given by an ab initio calculation.

# 1. INTRODUCTION

Collision-induced absorption in the region 20 - 900 $cm^{-1}$ has been measured in normal $H_2$ ($nH_2$) at 77.4 K and equilibrium $H_2$ ($eH_2$) and $eH_2$-He mixtures at 77.4, 195 and 292 K (ref. 1, hereinafter called I). The density of gas in this experiment was sufficiently low so that the collisions were mainly bimolecular. A semi-empirical line shape for such spectra has been developed and found to represent well the absorption in $H_2$ at 77.4 K from 20 to 500 $cm^{-1}$ in reference 2 (hereinafter called II). In this work we fit the measurements in I with the object of obtaining an analytical representation for these spectra for use in analyzing the far-infrared emission from planetary atmospheres containing $H_2$ and He.[3] Some of the problems in fitting these spectra are discussed.

Although the detailed analysis of these spectra is outside the scope of this work, we obtain the zeroth and first spectral moments and from these we obtain the range parameter in the induced dipole model for the isotropic overlap component of $H_2$-He.

## 2. THEORY OF SPECTRAL SHAPE

A semi-empirical approach to obtaining the shape of collision-induced lines based on assuming a reasonable and convenient form for the correlation function has been developed in I and reviewed in reference 4. The model correlation function satisfies certain mathematical and physical properties and its parameters are related to the moments of the spectrum. Although there is no guarantee that the resulting shape will fit the data, when it does it provides a very simple way of representing and analyzing such data.

The expression for the absorption coefficient of the translational-rotational spectrum due to quadrupole-induced and anisotropic overlap-induced dipoles in two-body encounters is given by

$$\alpha(\omega) = \frac{2\pi^2 n^2}{3\hbar c}\,\omega(1 - e^{-\beta\hbar\omega}) \sum_{JJ'} \rho_J (2J+1)(J2J';00)^2 \times \sum_{\lambda} S_\lambda \Gamma_\lambda (\omega - \omega_{JJ'}) \quad . \tag{1}$$

Here n is the number density of the single component gas, $\beta = (kT)^{-1}$, J is the angular momentum quantum number and $\omega_{JJ'}$ is the transition angular frequency, $\omega_{JJ'} = 2\pi c(\nu_{J'} - \nu_J)$. In practice, the density is frequently given in amagats, $\rho$, in which case $n = \rho n_0$, where $n_0$ is the number density at STP. The rotational energy levels (expressed in wavenumbers) are given by[5]

$$\nu_J = 59.3392J(J+1) - 0.04599J^2(J+1)^2 + 0.000052J^3(J+1)^3 \ \text{cm}^{-1} \quad . \tag{2}$$

The Boltzmann factor $\rho_J$ is given by

$$\rho_J = g_J e^{-\beta E_J} \Big/ \sum_J (2J+1) g_J e^{-\beta E_J} \quad , \tag{3}$$

where $E_J = hc\nu_J$ is the energy of rotational state J and the statistical factors due to nuclear spin are

$$g_J = 1, \ J \text{ even} \ ; \ g_J = 3, \ J \text{ odd} \quad .$$

The quantity $(2J+1)\rho_J$ for various energy levels is presented in Table 1.

Table 1. Population statistics for equilibrium hydrogen.

| J | $E_J/hc$ $cm^{-1}$ | $g_J$ | $(2J+1)\rho_J$ 77.4 K | 194.7 K | 292.4 K | normal hydrogen 77.4 K |
|---|---|---|---|---|---|---|
| 0 | 0 | 1 | 0.500 | 0.191 | 0.132 | 0.249 |
| 1 | 118.5 | 3 | 0.497 | 0.717 | 0.662 | 0.749 |
| 2 | 354.4 | 1 | 0.003 | 0.070 | 0.115 | 0.002 |
| 3 | 705.6 | 3 | - | 0.022 | 0.086 | - |
| 4 | 1168.9 | 1 | - | - | 0.004 | - |
| 5 | 1740.4 | 3 | - | - | 0.001 | - |
| para | | | 0.503 | 0.261 | 0.251 | 0.251 |
| ortho | | | 0.497 | 0.739 | 0.749 | 0.749 |

The induced translation-rotation spectrum of $H_2$ is due to quadrupole and anisotropic overlap-induced dipoles.[6,7] The type of contribution to a given transition is designated by the subscript $\lambda$. It is sufficient for our purpose here to assume that

$$\sum_\lambda S_\lambda \Gamma_\lambda(\omega-\omega_{JJ'}) = \Gamma(\omega-\omega_{JJ'}) \sum_\lambda S_\lambda \quad , \tag{4}$$

namely that the various contributions to a given transition may be represented by a single shape function, $\Gamma(\omega-\omega_{JJ'})$, with an intensity given by the sum of the various contributions which are discussed in the Appendix. The sum $\Sigma_\lambda S_\lambda$ which we designate by $S_q^{aa}$ is the total strength of the quadrupole-induced as well as the quadrupolar overlap-induced dipoles. The shape function is given by

$$\Gamma(\omega_-) = \frac{\tau_1}{\pi}\left[\exp\left(\frac{\tau_2}{\tau_1} + \frac{\beta\hbar\omega_-}{2}\right)\right]\frac{zK_1(z)}{1+\omega_-^2\tau_1^2} \quad , \tag{5}$$

with

$$z = \left[1+\omega_-^2\tau_1^2\right]^{\frac{1}{2}}\tau_3/\tau_1 \; ; \quad \tau_3^2 = \tau_2^2 + (\tfrac{1}{2}\beta\hbar)^2 \quad ,$$

$$\omega_- = \omega-\omega_{JJ'} \quad .$$

Here $K_1(z)$ is the modified Bessel function of the second kind with the properties,

$$zK_1(z) \to 1, \quad z \to 0,$$
$$K_1(z) \to (\pi/2z)^{\frac{1}{2}}e^{-z}, \quad z >> 1 \quad .$$

The time parameter $\tau_2$ controls the exponential decay of the wings. When $\tau_1 >> \tau_2$ the shape is Lorentzian in the vicinity of the transition frequency with a half-width given approximately by $\Delta\omega_1 = \tau_1^{-1}$. However, when $\tau_2/\tau_1 \sim 1$, as is true for $H_2$, (5) is never accurately Lorentzian and $\Delta\omega_1$ differs appreciably from the half-width that would be obtained by attempting to fit the data to a Lorentzian, as has been done in the past.[6]

The Clebsch-Gordan coefficients (J2J';00) are well known; their vanishing for $|J-J'| > 2$ and their symmetry,

$$(2J+1)(J2J';00)^2 = (2J'+1)(J'2J;00)^2 \quad , \tag{6}$$

allow us to write

$$\sum_{JJ'}\rho_J(2J+1)(J2J';00)^2\Gamma(\omega-\omega_{JJ'})$$
$$= A\Gamma(\omega) + \rho_0\Gamma(\omega-\omega_{02}) + \rho_2\Gamma(\omega+\omega_{02})$$
$$+ \frac{9}{5}\left[\rho_1\Gamma(\omega-\omega_{13}) + \rho_3\Gamma(\omega+\omega_{13})\right]$$
$$+ \frac{18}{7}\left[\rho_2\Gamma(\omega-\omega_{24}) + \rho_4\Gamma(\omega+\omega_{24})\right]$$
$$+ \frac{10}{3}\left[\rho_3\Gamma(\omega-\omega_{35}) + \rho_5\Gamma(\omega+\omega_{35})\right] + \cdots \tag{7}$$

with

$$A = \sum_J J(J+1)(2J+1)\rho_J/(2J-1)(2J+3) \quad . \tag{8}$$

In (7) the first term represents the translational band ($\omega_{JJ'} = 0$) while the others are the resonance ($\omega-\omega_{JJ'}$) and anti-resonance ($\omega+\omega_{JJ'}$) terms. This treatment neglects a small contribution to the absorption resulting from the anisotropy in the polarizability of $H_2$.[8]

For $H_2$-He collisions, the absorption coefficient becomes

$$\alpha_{ab}(\omega) = \frac{4\pi^2 n_a n_b}{3\hbar c}\omega(1-e^{-\beta\hbar\omega})\left[S_i^{ab}\Gamma_i(\omega)\right.$$
$$\left. + \sum_{JJ'}\rho_J(2J+1)(J2J';00)^2 S_q^{ab}\Gamma_q(\omega-\omega_{JJ'})\right] \quad . \tag{9}$$

The strength $S_q^{ab}$ represents the contributions to the intensity from quadrupolar and anisotropic overlap induction. These components are discussed in the Appendix. In (9), $n_a$ and $n_b$ are the densities of the components of the mixture. The term $S_i^{ab}\Gamma(\omega)$ represents the translational absorption due to the dipole induced in $H_2$-He collisions by isotropic overlap forces.[7] By symmetry such a contribution is impossible for rotational-translational transitions in $H_2$.

Equation (1) with (4) can be fitted with three parameters: two time constants $\tau_{1q}^{aa}$ and $\tau_{2q}^{aa}$ and a strength factor $S_q^{aa}$. Equation (9) can be fitted with six parameters: $\tau_{1q}^{ab}$, $\tau_{2q}^{ab}$ and $S_q^{ab}$ due to quadrupole and anisotropic induced dipoles and $\tau_{1i}^{ab}$, $\tau_{2i}^{ab}$ and $S_i^{ab}$ due to isotopic overlap-induced dipoles. The actual situation is even more complex, but the present data do not have sufficient precision to allow the quadrupolar and anisotropic overlap contributions to be resolved into separate components.

## 3. $H_2$-$H_2$ SPECTRA

The three-parameter least-squares fits of the $eH_2$-$H_2$ spectra, including the separate translational and rotational components, are shown in Figures 1 to 3, where we have plotted

$$D(\nu) = [\alpha(\nu)/\rho^2][\nu\tanh(\beta hc\nu/2)]^{-1} \qquad (10)$$

instead of $\alpha(\nu)/\rho^2$ to emphasize the translational band at the lower frequencies. The $J = 2 \leftarrow 0$ transition at 354.4 $cm^{-1}$ (S(0) line) and the $J = 3 \leftarrow 1$ transition at 587.1 $cm^{-1}$ (S(1) line) are partially resolved in the data. The $J = 4 \leftarrow 2$ transition at 814.5 $cm^{-1}$ (S(2) line) can be seen only as a distortion of the high frequency wing of the S(1) line at dry ice and room temperatures. Contributions to the absorption due to the molecular hexadecapole moment of $H_2$ and to double transitions, where both molecules change rotational state, are too small to make significant contributions to the spectrum and were omitted in the analysis. There is a trend at all temperatures for the fitted spectrum to exceed somewhat the experimental spectrum in the high frequency wing of the S(1) line. The values of the parameters $S_q^{aa}$, $\tau_{1q}^{aa}$ and $\tau_{2q}^{aa}$ are given in Table 2.

Table 2. Values of the parameters in (1), (4) and (5) used in fitting the experimental $H_2$ spectra. (n) signifies normal $H_2$ and (e) signifies equilibrium $H_2$.

| T (K) | $S_q^{aa}$ ($KA^{\circ 6}$) | $\tau_{1q}^{aa}$ ($10^{-14}$ s) | $\tau_{2q}^{aa}$ ($10^{-14}$ s) |
|---|---|---|---|
| 77.4 (n) | 106.3 ±0.8 | 10.26 ±0.14 | 3.91 ±0.25 |
| 77.4 (e) | 102.8 ±0.6 | 10.23 ±0.13 | 4.20 ±0.25 |
| 195 (e) | 129.5 ±0.5 | 5.95 ±0.07 | 2.59 ±0.13 |
| 292 (e) | 149.7 ±2.4 | 4.48 ±0.22 | 2.12 ±0.47 |

A similar least-squares fit to the normal hydrogen spectrum (not shown) observed at 77.4 K was made. The agreement of the results at 77.4 K between $nH_2$ (para-ortho distribution, 1:2.98) and $eH_2$ (para-ortho distribution, 1:1)

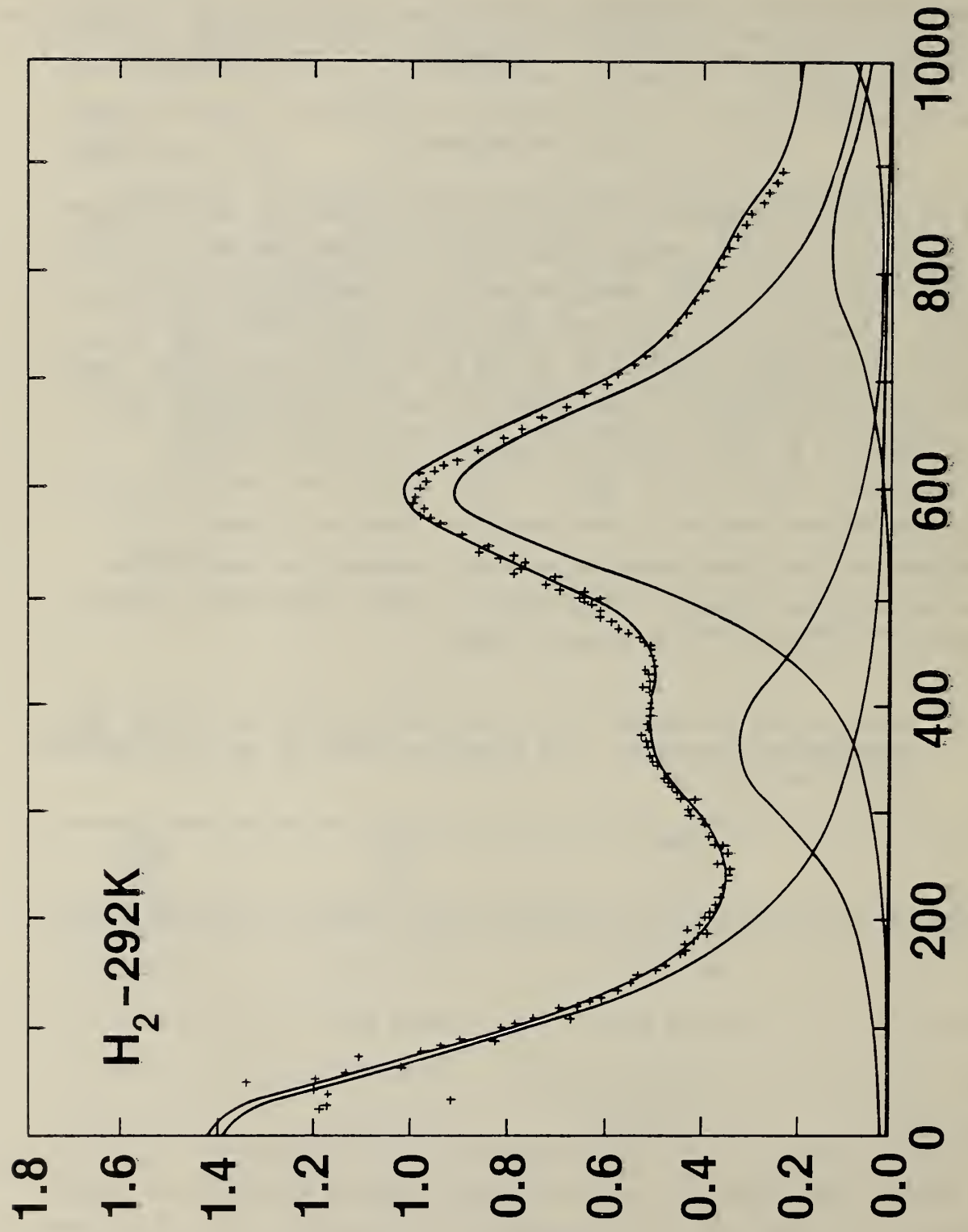


Figure 1. $eH_2$, 292 K. Three-parameter least-squares fit of $D_{aa}(\nu)$, defined by (10).

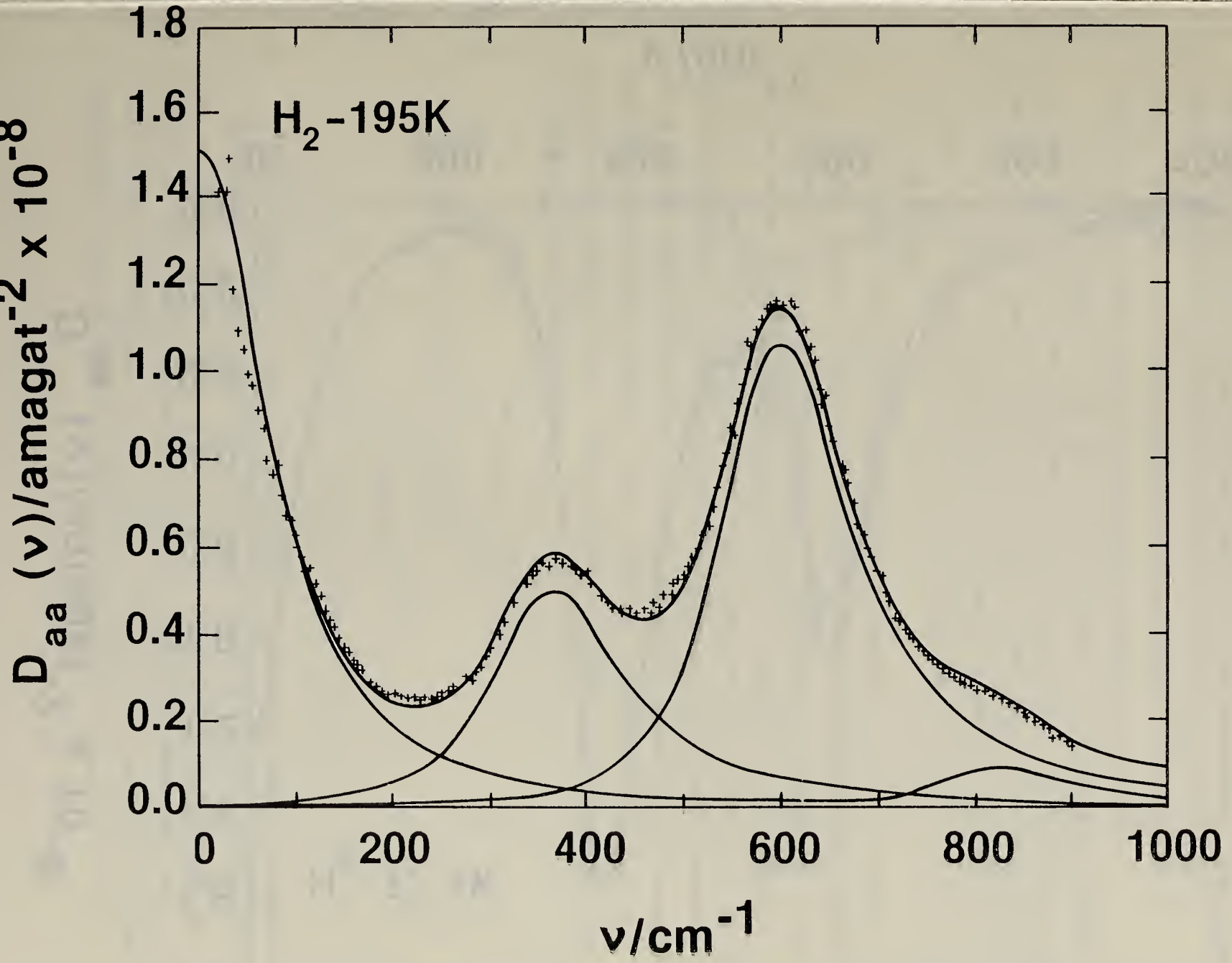


Figure 2. $eH_2$, 195 K. Three-parameter least-squares fit of $D_{aa}(\nu)$, defined by (10).

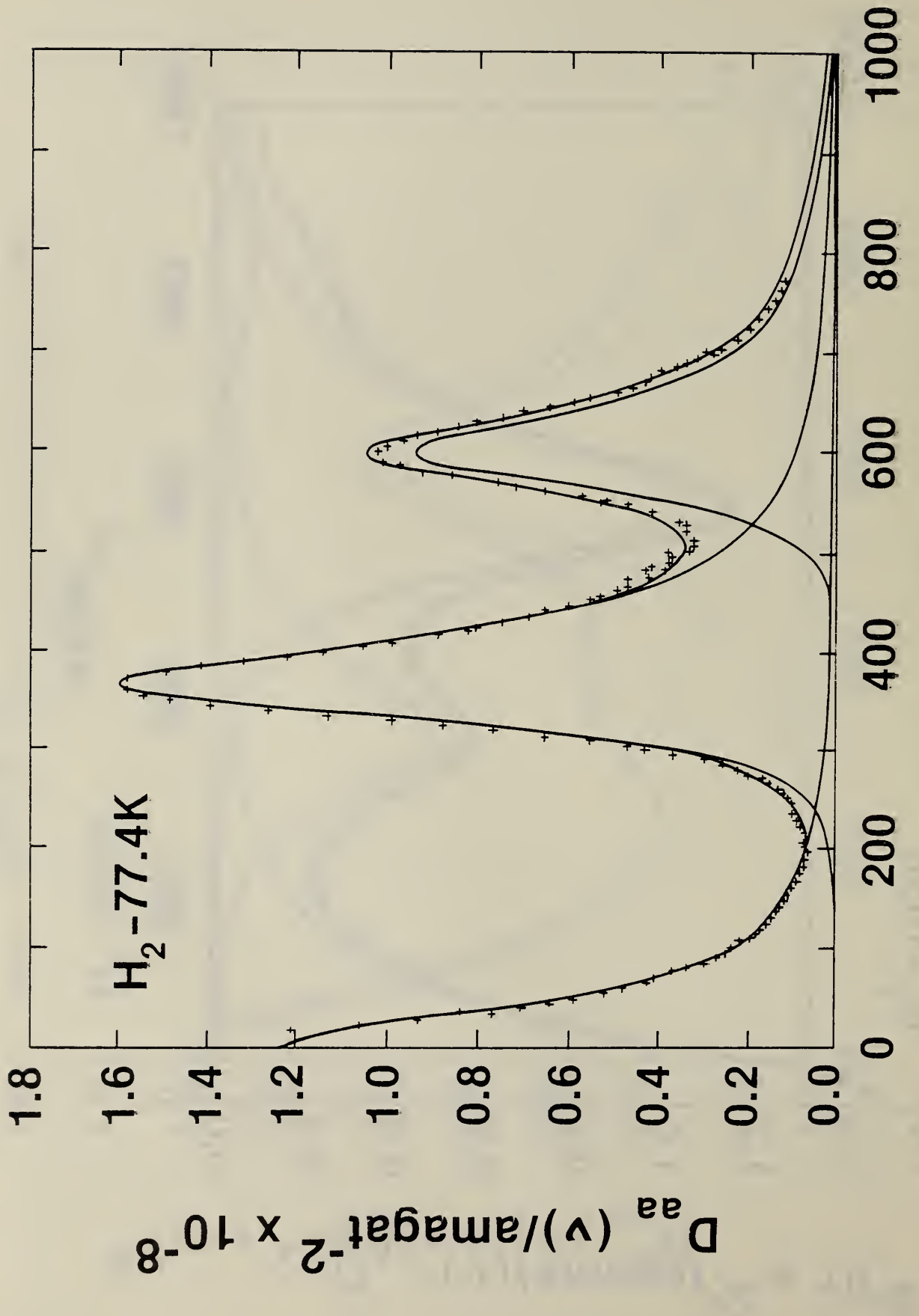


Figure 3. $eH_2$, 77.4 K. Three-parameter least-squares fit of $D_{aa}(\nu)$, defined by (10).

confirms that the normal population (equilibrated at 292 K) was preserved at the lower temperature (77.4 K) and that the equilibrium population (equilibrated at 77.4 K) was indeed achieved in the measurement. The three percent difference in the intensity factor S in the two measurements at 77.4 K confirms that the gas densities were determined consistently to within an error which could not have greatly exceeded one percent.

Other adjustments to the data have been made in which we have allowed the time constants to be different for the translational and rotational bands. However, this introduces very little change in the adequacy of the adjustment. In general, the differences in the two values of $\tau_1$ and $\tau_2$, taking into account the statistical correlation which exists between the values, is not statistically significant.

We believe the accuracy of the fitted parameters to be of the order of 5%, although relative values and the temperature dependence may be more reliable. Up to this point our analysis is independent of any models of the intermolecular potential. We can evaluate the integrals $I_8(T)$, $I'(\sigma/\rho,T)$ and $I''(\sigma/\rho,T)$ introduced in the Appendix only if we know the correct form of the (quantum mechanical) distribution function g(x) as well as the parameters $\sigma$ and $\varepsilon$ of the Lennard-Jones model, or the equivalent parameters of whatever more accurate potential model is used. However, for our purpose here we present only empirical fits. From the data in Table 2, we can express the strength $S_q^{aa}$ by the expression

$$S_q^{aa} = 142(T/T_0)^{0.26}\ \text{KÅ}^6$$

with $T_0 = 273.15$ K. Similarly we find

$$\tau_{1q}^{aa} = 4.85(T/T_0)^{-0.593} \cdot 10^{-14}\ \text{s}$$

$$\tau_{2q}^{aa} = 2.17(T/T_0)^{-0.523} \cdot 10^{-14}\ \text{s} \quad .$$

Theory leads one to expect[2] the product $\tau_1\tau_2 T$ to be roughly independent of temperature, varying only as $I_8(T)/I_{10}(T)$ assuming that the quadrupole-induced dipole predominates. For a classical Lennard-Jones potential, an analysis of the asymptotic behavior of the $I_n$ integrals shows that this ratio varies from a $T^0$ dependence at low temperatures ($\varepsilon \gg kT$) to $T^{-1/6}$ at high temperatures. The observed variation from the above fittings is $T^{-0.12}$.

## 4. THE REDUCED $H_2$-He SPECTRA

The experimental and fitted spectra at 77, 195 and 292 K, are shown in Figures 5 to 7 for the reduced $H_2$-He spectra, where we have plotted

$$D_{ab}(\nu) = (\rho_m^2/\rho_a\rho_b)D_m(\nu) - (\rho_a/\rho_b)D_{aa}(\nu) \quad . \tag{11}$$

The spectral function $D(\nu)$ is defined by (10) and the subscript m refers to the mixture whose density is given by $\rho_m = \rho_a + \rho_b$. Also shown are the separate isotropic overlap and quadrupole-induced components. The fitted parameters are given in Table 3. It appears that the discrepancies between the fitted and measured reduced spectra for $H_2$-He may be attributed to the inaccuracy in the experimental results. As explained in I, this arises in the case of $H_2$-He mixtures with too high an $H_2$ concentration which yields $\alpha_{ab}(\nu)$ as a small difference between two large numbers.

Table 3. Values of the parameters in (9) (4) and (5) used in fitting the reduced e$H_2$-He spectra.

| | Isotropic Overlap | | | Quadrupolar Plus Anisotropic Overlap | | |
|---|---|---|---|---|---|---|
| T | $S_i^{ab}$ | $\tau_{1i}^{ab}$ | $\tau_{2i}^{ab}$ | $S_q^{ab}$ | $\tau_{1q}^{ab}$ | $\tau_{2q}^{ab}$ |
| (K) | ($KA^{\circ 6}$) | ($10^{-14}$ s) | ($10^{-14}$ s) | ($KA^{\circ 6}$) | ($10^{-14}$ s) | ($10^{-14}$ s) |
| 77.4 | 34.47 | 3.64 | 4.66 | 6.93 | 7.02 | 13.44 |
| 195 | 81.34 | 1.99 | 4.22 | 19.14 | 4.13 | 2.38 |
| 292 | 119.1 | 1.91 | 2.52 | 21.0 | 4.20 | 2.86 |

The rapid decrease in $D_{ab}(\nu)$ at low frequencies at 195 and 292 K might be attributed to the inter-collisional interference effect.[9] However, an analysis of the data shows that these dips are probably not statistically significant. It should be noted that dividing $\alpha(\nu)$ by $\nu\tanh(\beta hc\nu/2)$ to obtain $D(\nu)$ greatly amplifies any errors in the low frequency data.

On comparing the $H_2$ spectra (Figures 1 to 3) with the reduced $H_2$-He spectra (Figures 4 to 6) we note that translational band intensity of the

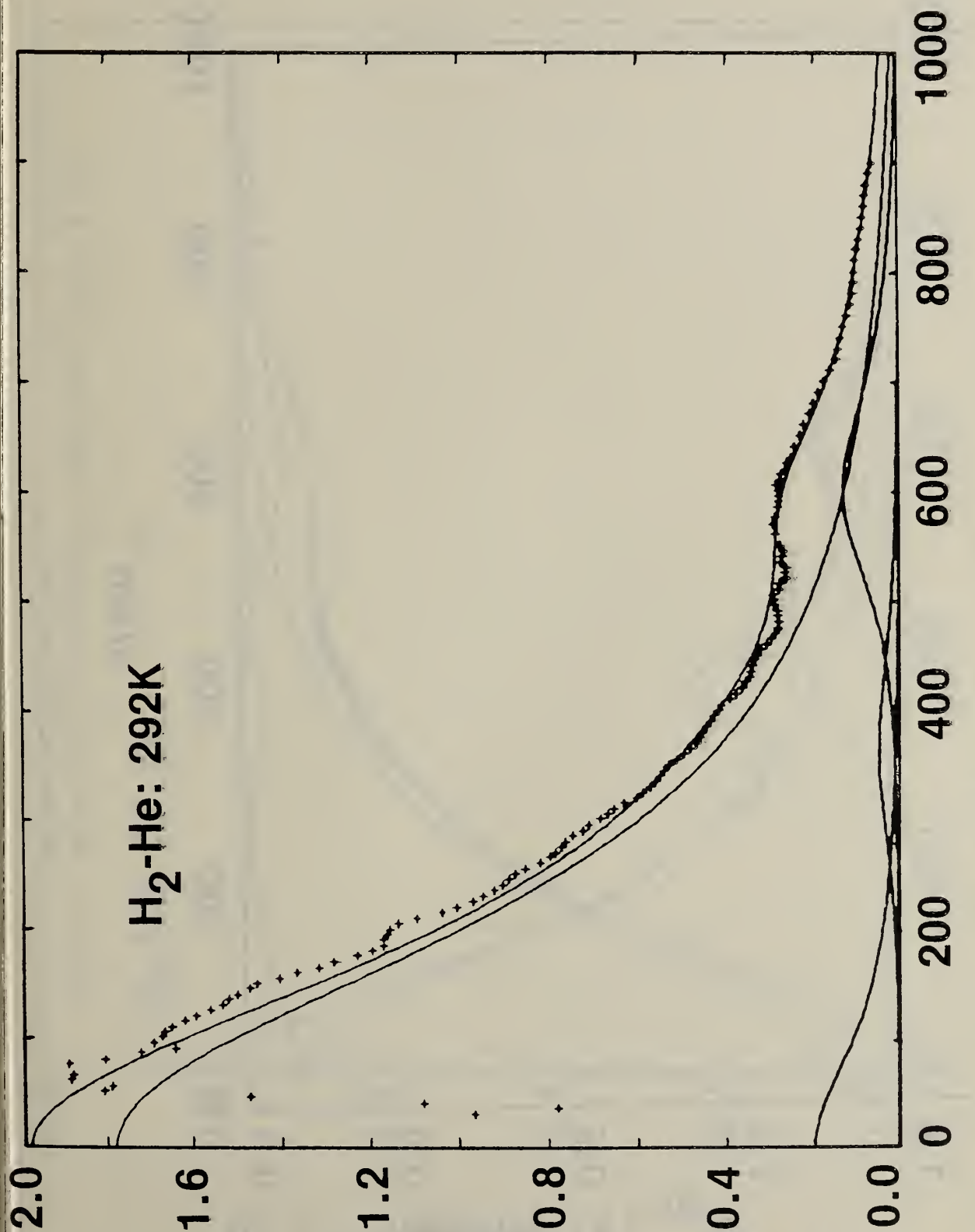


Figure 4. e$H_2$-He, 292 K. Six-parameter least-squares fit of $D_{ab}(\nu)$, defined by (10) and (11).

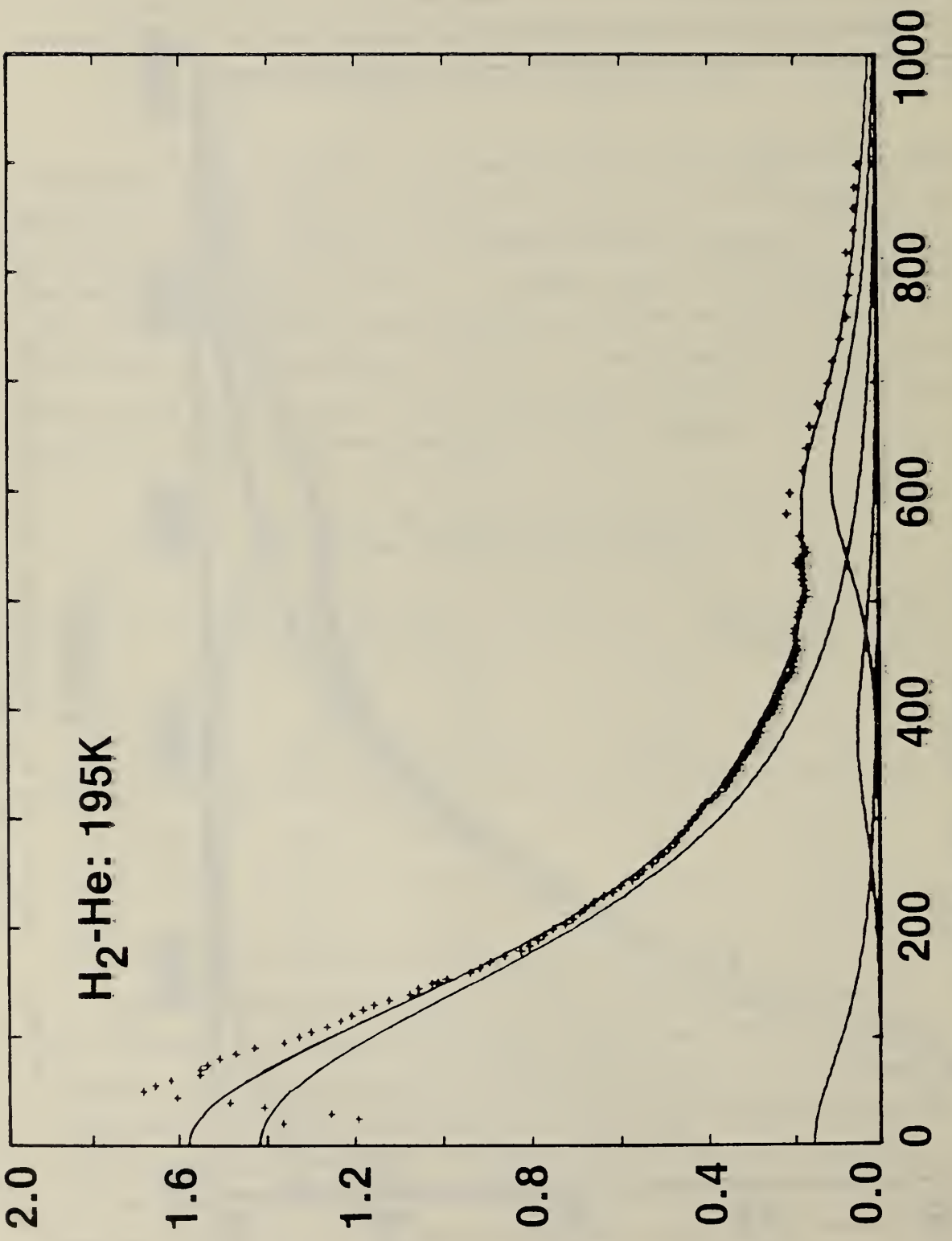


Figure 5. $eH_2$-He, 195 K. Six-parameter least-squares fit of $D_{ab}(\nu)$, defined by (10) and (11).

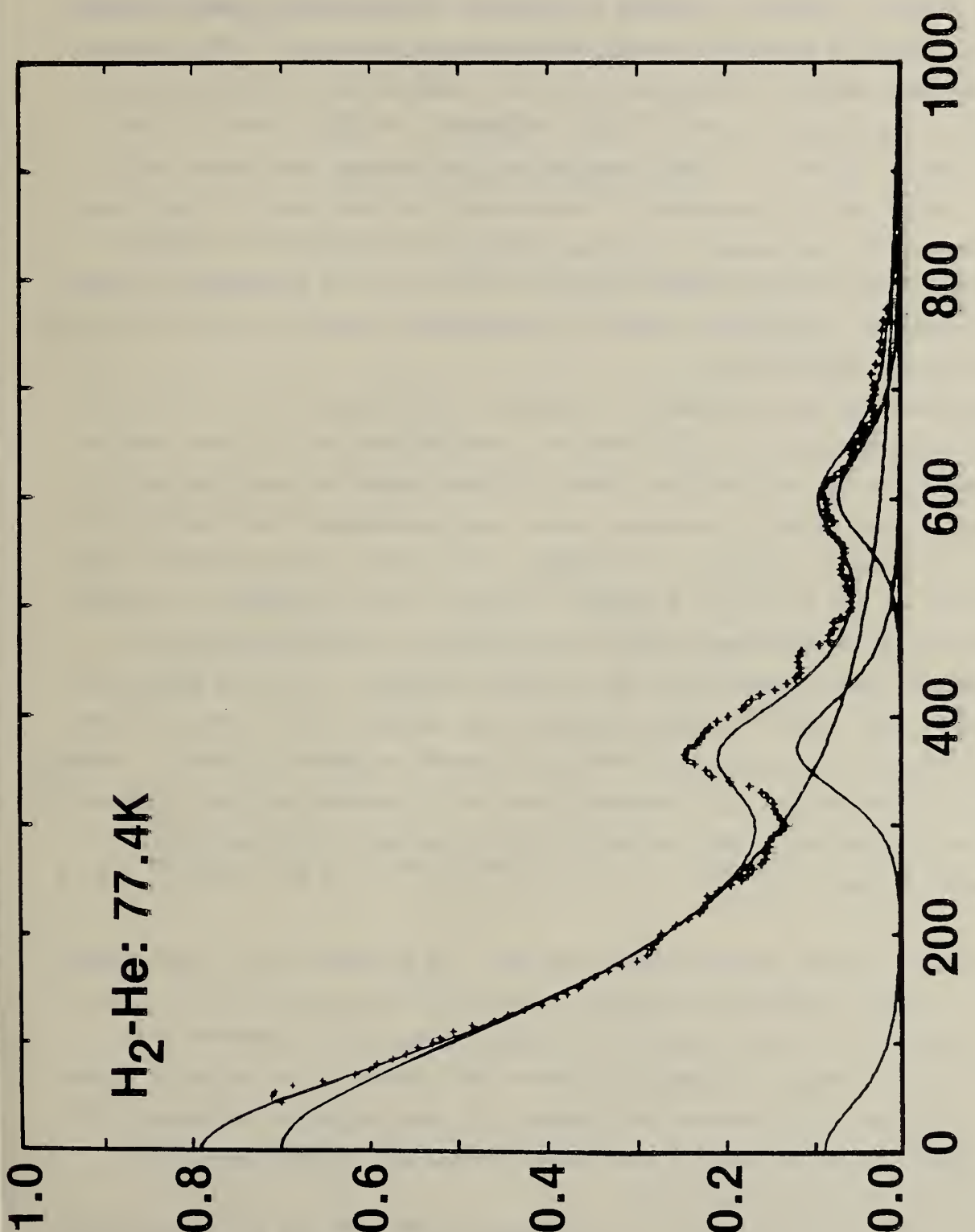


Figure 6. $eH_2$-He, 77.4 K. Six-parameter least-squares fit of $D_{ab}(\nu)$, defined by (10) and (11).

latter is much greater than that of the former. This is due to the isotropic overlap induction in $H_2$-He collisions. On the other hand, the S(0) and S(1) lines in $H_2$-He have much less intensity than in $H_2$. This results from the much smaller polarizability of He compared with $H_2$ which greatly reduces the quadrupole-induced dipole component. Finally, the S(0) and S(1) lines in $H_2$-He at a given temperature are broader than those in $H_2$. Such a result may be understood if anisotropic overlap makes a significant contribution to the intensity of these lines. The width of an overlap component should be considerably greater than that of a quadrupolar-induced line because of the shorter range and consequently shorter collision duration of the former interaction.

Undoubtedly the inaccuracy in the data contributed to our difficulty in obtaining a unique set of parameters from the fitting. It was surprising, nevertheless, to find that these fittings showed so much flexibility and that a wide range of parameter sets could approximate the experimental curves with equal accuracy. For example, the overall rms fractional error in the fit at 195 K is only 8 percent. However, the adjustment is statistically loose and the least squares fit shows very strong correlation between the time constants and the strength parameter. One can adjust for changes in the former by making compensating changes in the latter. Thus, the quadrupolar and anisotropic-overlap strength parameter S shows a standard error of 25 percent, $\tau_1\tau_2$ a standard error of 50 percent and $\tau_2/\tau_1$ a standard error of 200 percent. The isotropic overlap parameters are much more precisely defined: $\tau_{1i}^{ab}\tau_{2i}^{ab} = 8.4 \pm 1.1$, $\tau_{2i}^{ab} \Big/ \tau_{1i}^{ab} = 2.1 \pm 0.5$ and $S_i^{ab} = 81.3 \pm 5.1$.

Apart from the imprecision of the data, we believe that a six-parameter fit to a rather featureless spectrum such as $H_2$-He, particularly at 195 and 292 K, provides too many degrees of freedom unless the parameters are restricted by theory. Attempts to reduce the number of variables by invoking a relation in II between the product $\tau_1\tau_2$ and molecular parameters was frustrated in part because of the unknown admixture of quadrupole and anisotropic overlap interactions.

Since as explained above, the parameters $S_q^{ab}$, $\tau_{1q}^{ab}$ and $\tau_{2q}^{ab}$ are not well defined, there is little to be gained by trying to determine the temperature

dependence of the quadrupolar parameters. The isotropic parameters, however, can be fitted with reasonable accuracy to yield

$$S_i^{ab} = 112(T/T_o)^{0.93}\ \text{KÅ}^6$$

$$\tau_{1i}^{ab} = 1.74(T/T_o)^{-0.54}\cdot 10^{-14}\ \text{s}$$

$$\tau_{2i}^{ab} = 3.4(T/T_o)^{-0.30}\cdot 10^{-14}\ \text{s} \quad .$$

## 5. SPECTRAL MOMENT ANALYSIS

We can obtain immediately from the parameters of the fitted spectrum the experimental invariants,

$$\alpha_{aa} = n^{-2} \int_0^\infty \alpha_{aa}(\omega) d\omega \quad , \tag{12}$$

$$\gamma_{aa} = \frac{\beta\hbar}{2} n^{-2} \int \frac{\alpha_{aa}(\omega) d\omega}{\omega \tanh(\beta\hbar\omega/2)} \quad . \tag{13}$$

Thus, following the derivation of (31b) and (35) in II we obtain

$$\alpha_q^{aa} = \gamma_q^{aa} \left( \frac{6kT}{I} + \frac{1}{\tau_{1q}^{aa} \tau_{2q}^{aa}} \right) \tag{14}$$

for quadrupole and anisotropic overlap-induced dipoles. From (1), (4) and (13) we find that

$$\gamma_q^{aa} = \frac{\pi^2}{3kTc} S_q^{aa} \quad . \tag{15}$$

The quantity $\gamma_q^{aa}(6kT/I)$ is the contribution to $\alpha_{aa}$ from the rotational transitions $\Delta J_1 = \pm 2$, $\Delta J_2 = 0$, while $\gamma_q^{aa} \Big/ \tau_{1q}^{aa} \tau_{2q}^{aa}$ is the translational contribution.

For the reduced $H_2$-He spectrum, (12) to (15) apply, where aa is replaced by ab for the quadrupole and anisotropic overlap-induced contribution and $n^2$ is replaced by $n_a$ and $n_b$. There is, in addition, the isotropic overlap contribution for which

$$\alpha_i^{ab} = \gamma_i^{ab} \Big/ \tau_{1i}^{ab} \tau_{2i}^{ab} \quad , \quad \gamma_i^{ab} = \frac{2\pi}{3kTc} S_i^{ab} \tag{16}$$

and

$$\alpha_{ab} = \alpha_q^{ab} + \alpha_i^{ab} \quad , \quad \gamma_{ab} = \gamma_q^{ab} + \gamma_i^{ab} \quad . \tag{17}$$

Table 4 gives the various values of $\gamma$ computed from (15) and the values of S given in Table 2. Table 5 gives the values of (6kT/I) and $(\tau_1\tau_2)^{-1}$. We see from Tables 4 and 5 that the translational contribution to $\alpha_q^{aa}$ is between 15 and 17 percent depending on the temperature.

Table 4. Values of $\gamma$ defined by (13). $\gamma_q^{aa}$ is due to $H_2$-$H_2$ collisions, $\gamma_i^{ab}$ is due to isotropic overlap induction in $H_2$-He collisions and $\gamma_q^{ab}$ is due to quadrupolar and anisotropic overlap induction in $H_2$-He collisions.

| T (K) | $\gamma_q^{aa}$ $10^{-58}$ s cm$^5$ | $\gamma_i^{ab}$ $10^{-58}$ s cm$^5$ | $\gamma_q^{ab}$ $10^{-58}$ s cm$^5$ |
|---|---|---|---|
| 77.4 (n) | 3.012 | -- | -- |
| 77.4 (e) | 2.913 | 1.954 | 0.3928 |
| 195 (e) | 1.458 | 1.834 | 0.4312 |
| 292 (e) | 1.123 | 1.786 | 0.3150 |

Table 5. Values of $\alpha_q^{aa}$, (6kT)/I which is proportional to the rotational contribution and $\left(\tau_{1q}^{aa}\tau_{2q}^{aa}\right)^{-1}$ which is proportional to the translational contribution to $\alpha_q^{aa}$ in $H_2$-$H_2$ collision.

| T (K) | (6kT)/I ($10^{28}$ s$^{-2}$) | $\left(\tau_{1q}^{aa}\tau_{2q}^{aa}\right)^{-1}$ ($10^{28}$ s$^{-2}$) | $\alpha_q^{aa}$ ($10^{-31}$ s$^{-1}$ cm$^5$) |
|---|---|---|---|
| 77.4 (n) | 0.1360 | 0.02493 | 4.847 |
| 77.4 (e) | 0.1360 | 0.02327 | 4.640 |
| 195 (e) | 0.3421 | 0.06489 | 5.934 |
| 292 (e) | 0.5138 | 0.1053 | 6.953 |

In I, $\alpha_q^{aa}$ and $\gamma_q^{aa}$ were evaluated from data in the region 20 to 900 cm$^{-1}$ and from data from 900 to 1600 cm$^{-1}$ obtained elsewhere.[10] It was necessary, however, to adjust the data of the latter experiment to agree with the results in I by forcing a fit in the overlapping region 800 to 900 cm$^{-1}$. The present values of $\gamma_q^{aa}$ are within 0.2 percent of those obtained in I. The present $\alpha_q^{aa}$ at 77 K is less than that in I by 4 percent and at 195 K and 292 K it is greater than the values given in I by about 1.3 percent.

As is evident from the spectral fits for the reduced $H_2$-He spectrum (Figures 4-6), the isotropic overlap contribution is dominant. Table 4 shows that $\gamma_i^{ab}$, the isotropic overlap contribution, is on the average 5 times greater than that due to quadrupole and anisotropic overlap induction $\gamma_q^{ab}$. A comparison of $\alpha_i^{ab}$ and $\alpha_q^{ab}$ shows that $\alpha_i^{ab} \approx 6\alpha_q^{ab}$.

To proceed one step further with our analysis, we can immediately obtain the range of the isotropic overlap-induced dipole, $\rho_{ov}$, from[2]

$$\rho_{ov}^2 = \frac{kT}{m} \tau_{1i}^{ab}\tau_{2i}^{ab} \left[1 + 2 \frac{I_\Omega}{I_R} \left(\frac{\rho_{ov}}{\sigma}\right)^2\right] . \qquad (18)$$

Here m is the reduced mass and $I_\Omega$ and $I_r$ are integrals involving the radial distribution function defined in II. Since $(\rho_{ov}/\sigma)^2 << 1$, only an approximate evaluation of $I_\Omega/I_R$ is necessary and $I_\Omega \approx I_R$ is a valid first approximation.

Using $\sigma$ = 2.77 Å and m = 1.34 amu = $2.226 \cdot 10^{-24}$ g for the reduced mass of $H_2$-He, we find from the data given in Table 6 that $\rho_{ov}$ = 0.288 Å at 77 K, 0.323 Å at 194 K and 0.299 Å at 292 K. The average is 0.303 Å which is in satisfactory agreement with the value $\rho_{ov}$ = 0.324 Å given by an ab initio calculation.[11]

Table 6. Values of $(\tau_{1q}^{ab}\tau_{2q}^{ab})^{-1}$, $\alpha_q^{ab}$, $(\tau_{1i}^{ab}\tau_{2i}^{ab})^{-1}$ and $\alpha_i^{ab}$ for $H_2$-He collisions, where $(\tau_1\tau_2)^{-1}$ is proportional to the translational contribution of $\alpha_{ab}$.

| T (K) | $(\tau_{1q}^{ab}\tau_{2q}^{ab})^{-1}$ ($10^{28}$ $s^{-2}$) | $\alpha_q^{ab}$ ($10^{-31}$ $s^{-1}$ $cm^5$) | $(\tau_{1i}^{ab}\tau_{2i}^{ab})^{-1}$ ($10^{28}$ $s^{-2}$) | $\alpha_i^{ab}$ ($10^{-31}$ $s^{-1}$ $cm^5$) |
|---|---|---|---|---|
| 77.4 | 0.0106 | 0.576 | 0.0590 | 3.810 |
| 195 | 0.1017 | 1.914 | 0.1191 | 8.458 |
| 292 | 0.0833 | 1.880 | 0.2078 | 12.89 |

## 6. Conclusions

The far infrared absorption spectra of $H_2$-$H_2$ and $H_2$-He collisions have been fitted with a semi-empirical line shape. For $H_2$-$H_2$ the results appear to be satisfactory; for $H_2$-He the fit is less good. In $H_2$-$H_2$ collisions only a single quadrupolar component was needed to fit the experimental data. The strength and the time constants of this line shape due to unresolved pure quadrupole plus quadrupolar overlap components have been fitted by an empirical power law temperature dependence which will allow the data to be conveniently interpolated for temperatures in the range 70 - 300 K. However, data at additional temperatures would be very useful in establishing the accuracy of these empirical power laws. The strength, $S_q^{aa}$, can be resolved into quadrupole and overlap contributions if one uses independent information on the $H_2$ quadrupole moment and intermolecular potential.

The $H_2$-He spectra were determined less accurately since the observed spectrum of the mixture is the sum of the $H_2$-$H_2$ and the $H_2$-He contributions. In $H_2$-He the dominant interaction is isotropic, and although the quadrupolar component is easily seen, the accuracy with which it has been separated from the $H_2$-$H_2$ quadrupolar absorption is poor. Therefore, only the isotropic overlap parameters have been fitted to an interpolating temperature dependence. Data extending to higher frequencies (up to 2000 $cm^{-1}$)[12] may improve the accuracy with which the parameters of the quadrupolar component can be determined.

## 7. Acknowledgments

The authors thank Dr. G. S. Orton and Mr. V. G. Kunde for helpful discussions.

This report was prepared for the Jet Propulsion Laboratory, California Institute of Technology, under contract NAS 7-100, sponsored by the PLANETARY ATMOSPHERES PROGRAM OFFICE, OFFICE of SPACE SCIENCE, NATIONAL AERONAUTICS and SPACE ADMINISTRATION.

# APPENDIX

The R-dependence of the induced-dipole in $H_2$ may be obtained from the work of Poll and Van Kranendonk[7] and is given by

$$\left|\mu(R)\right|^2 = 2\left(\left[\sqrt{3}\,\frac{\alpha\Theta}{R^4} + \mu_3(R)\right]^2 + \mu_1^2(R)\right) \quad . \tag{A1}$$

Here $\sqrt{3}\alpha\Theta R^{-4}$ is the quadrupole-induced dipole, $\alpha = \frac{1}{3}\,(\alpha_{\parallel} + 2\alpha_{\perp})$ is the average polarizability and R is the intermolecular separation. The quadrupole moment, $\Theta$, is defined by $\Theta = \int \rho_e(r)\left[z^2 - \frac{1}{2}\,(x^2 + y^2)\right] 4\pi r^2 dr$ where $\rho_e(r)$ is the charge density in the molecule. The induced dipoles $\mu_3(R)$ and $\mu_1(R)$ are due to an anisotropic overlap interaction and are assumed to be represented by

$$\mu_3(R) = \mu_3^0 e^{(\sigma-R)/\rho_1} \tag{A2}$$

$$\mu_1(R) = \mu_1^0 e^{(\sigma-R)/\rho_2} \tag{A3}$$

where $\mu^0$ is the magnitude at $R = \sigma$, $\rho$ is a range parameter and $\sigma$ is a molecular diameter. The induced dipoles $\mu_3(R)$ and $\mu_1(R)$ arise from terms with different rotational symmetry such that the former can interfere with the quadrupole-induced dipole whereas the latter cannot.[7] The factor of 2 in (A1) is due to the induction of a dipole in molecule a by molecule b and vice versa.

The strength parameter S is given by

$$S = \int_0^\infty g(R)\,\left|\mu(R)\right|^2\,4\pi R^2 dR \quad , \tag{A4}$$

where g(R) is the radial distribution function.

With the dipole given by (A1) we find

$$S_q^{aa} = 2\left(\frac{3\alpha^2\Theta^2}{\sigma^5}\,I_8 + \frac{2\sqrt{3}\alpha\Theta\mu_3^0}{\sigma}\,I'(\sigma/\rho_3) + \sigma^3(\mu_3^0)^2 I''(\sigma/\rho_3) + \sigma^3(\mu_1^0)^2 I''(\sigma/\rho_1)\right) \quad . \tag{A5}$$

The integrals I are defined by

$$I_8 = \int_0^\infty g(x)x^{-8}4\pi x^2 dx \quad , \tag{A6}$$

$$I'(\sigma/\rho) = \int_0^\infty g(x)x^{-4}e^{-(x-1)\sigma/\rho}4\pi x^2 dx \quad , \tag{A7}$$

$$I''(\sigma/\rho) = \int_0^\infty g(x)e^{-2(x-1)\sigma/\rho}4\pi x^2 dx \quad . \tag{A8}$$

If the overlap is sufficiently small, only the first two terms in (A5) will be significant, namely, the contribution due to the quadrupole-induced dipole and the term resulting from the interference between this dipole and $\mu_3(R)$.

In $H_2$-He collisions involving the quadrupole and anisotropic-induced dipoles, the strength factor is

$$S_q^{ab} = \left(\frac{3\alpha_b^2\Theta_a^2}{\sigma_{ab}^5}\right) I_8 + \frac{2\sqrt{3}\alpha_b\Theta_a\mu_3^0}{\sigma_{ab}} I'(\sigma_{ab}/\rho_3)$$

$$+ \sigma_{ab}^3(\mu_3^0)^2 I''(\sigma_{ab}/\rho_3) + \sigma_{ab}^3(\mu_1^0)^2 I''(\sigma_{ab}/\rho_1) \quad , \tag{A9}$$

where $\Theta_a$ is the quadrupole moment of $H_2$, $\alpha_b$ is the polarizability of He, $\sigma_{ab}$ is the molecular diameter for $H_2$-He collisions and the factor of 2 is not present because $\Theta_b = 0$. In collisions between two different particles, there is, in addition to the induced dipoles presented previously which produce rotational-translational transitions, an induced isotropic overlap dipole which produces only translational transitions. This is given by

$$S_i^{ab} = \sigma_{ab}^3(\mu_i^0)^2 I''(\sigma_{ab}/\rho_{ov}) \quad , \tag{A10}$$

when the isotropic overlap dipole is assumed to have the form

$$\mu_{ov}(R) = \mu_i^0 e^{(\sigma_{ab}-R)/\rho_{ov}} \quad . \tag{A11}$$

## REFERENCES


1. G. Birnbaum, J. Quant. Spectrosc. Radiat. Transfer 19, 51 (1978).
2. G. Birnbaum and E. R. Cohen, Can. J. Phys. 54, 593 (1976).
3. R. Hanel, B. Conrath, M. Flasar, V. Kunde, P. Lowman, W. Maguire, J. Pearl, J. Pirraglia, R. Samuelson, D. Gautier, P. Gierasch, S. Kumar and C. Ponnampesuma, Science 204, 972 (1979).
4. G. Birnbaum, Italian Physical Soc., E. Fermi International School of Physics, "Intermolecular Spectroscopy and Dynamical Properties of Dense Systems," edited by J. Van Kranendonk, Italian Physical Society, 75 111 (1980).
5. B. P. Stoicheff, Can. J. Phys. 35, 730 (1957).
6. For a discussion of collision-induced absorption in $H_2$ and $H_2$-rare gas mixtures see H. Welsh, Intl. Rev. Science 3, 33, Buttersworths, London (1972).
7. J. D. Poll and J. Van Kranendonk, Can. J. Phys. 39, 189 (1961).
8. J. Van Kranendonk and Z. J. Kiss, Can. J. Phys. 37, 1187 (1959).
9. J. Van Kranendonk, Can. J. Phys. 46, 1173 (1968).
10. J. W. Mactaggart and J. L. Hunt, Can. J. Phys. 47, 65 (1969).
11. P. E. S. Wormer and G. Van Dijk, J. Chem. Phys. 70, 5695 (1979).
12. G. Birnbaum, G. Bachet, E. R. Cohen and P. Dore (to be published).

NBS-114A (REV. 9-78)

| U.S. DEPT. OF COMM. BIBLIOGRAPHIC DATA SHEET | 1. PUBLICATION OR REPORT NO. NBSIR 80-2175 | 2. Gov't. Accession No. | 3. Recipient's Accession No. |
|---|---|---|---|

**4. TITLE AND SUBTITLE**

Analysis of the Shape of the Far-Infrared Spectra of $H_2$-$H_2$ and $H_2$-He Collisions

**5. Publication Date**

April 1981

**6. Performing Organization Code**

**7. AUTHOR(S)**

E. Richard Cohen and George Birnbaum

**8. Performing Organ. Report No.**

**9. PERFORMING ORGANIZATION NAME AND ADDRESS**

NATIONAL BUREAU OF STANDARDS
DEPARTMENT OF COMMERCE
WASHINGTON, DC 20234

**10. Project/Task/Work Unit No.**

**11. Contract/Grant No.**

**12. SPONSORING ORGANIZATION NAME AND COMPLETE ADDRESS** *(Street, City, State, ZIP)*

**13. Type of Report & Period Covered**

**14. Sponsoring Agency Code**

**15. SUPPLEMENTARY NOTES**

☐ Document describes a computer program; SF-185, FIPS Software Summary, is attached.

**16. ABSTRACT** *(A 200-word or less factual summary of most significant information. If document includes a significant bibliography or literature survey, mention it here.)*

The collision-induced far-infrared spectra due to $H_2$-$H_2$ and $H_2$-He collisions have been previously measured in the range 20 to 900cm$^{-1}$ at 77.4, 194.7 and 292.4 K. These spectra are fitted with a semi-empirical line shape and the parameters in the shape function are evaluated. The accuracy of these fitting is discussed. The zeroth and first spectral moments for the isotropic overlap translational spectrum due to $H_2$-He collisions are obtained and give a value for the range parameter in the induced-dipole function in good agreement with that given by an *ab initio* calculation.

**17. KEY WORDS** *(six to twelve entries; alphabetical order; capitalize only the first letter of the first key word unless a proper name; separated by semicolons)*

Band shape analysis; collision-induced absorption; far infrared; $H_2$-$H_2$ collisions; $H_2$-He collisions; planetary atmospheres; quadrupole-induced absorption; spectral moments.

**18. AVAILABILITY**

☒ Unlimited

☐ For Official Distribution. Do Not Release to NTIS

☐ Order From Sup. of Doc., U.S. Government Printing Office, Washington, DC 20402, SD Stock No. SN003-003-

☒ Order From National Technical Information Service (NTIS), Springfield, VA. 22161

| 19. SECURITY CLASS (THIS REPORT) | 21. NO. OF PRINTED PAGES |
|---|---|
| UNCLASSIFIED | 25 |
| **20. SECURITY CLASS (THIS PAGE)** | **22. Price** |
| UNCLASSIFIED | 5.00 |

USCOMM-DC